doi:10.1016/j.jmb.2008.01.002 J. Mol. Biol. (2008) 377, 854–869

JMB

Available online at www.sciencedirect.com

ScienceDirect

ELSEVIER

Yeast Cytosine Deaminase Mutants with Increased Thermostability Impart Sensitivity to 5-Fluorocytosine

Tiffany S. Stolworthy[1]†, Aaron M. Korkegian[2]†, Candice L. Willmon[1], Andressa Ardiani[3], Jennifer Cundiff[1], Barry L. Stoddard[2] and Margaret E. Black[1,3]*

[1]*Department of Pharmaceutical Sciences, Washington State University, Pullman, WA 99164-6534, USA*

[2]*Fred Hutchinson Cancer Research Center and the Graduate Program in Molecular and Cell Biology, University of Washington, 1100 Fairview Avenue North A3-023, Seattle, WA 98109, USA*

[3]*School of Molecular Biosciences, Washington State University, Pullman, WA 99164-6534, USA*

Received 14 September 2007; received in revised form 29 December 2007; accepted 2 January 2008
Available online
11 January 2008

Edited by I. Wilson

Prodrug gene therapy (PGT) is a treatment strategy in which tumor cells are transfected with a 'suicide' gene that encodes a metabolic enzyme capable of converting a nontoxic prodrug into a potent cytotoxin. One of the most promising PGT enzymes is cytosine deaminase (CD), a microbial salvage enzyme that converts cytosine to uracil. CD also converts 5-fluorocytosine (5FC) to 5-fluorouracil, an inhibitor of DNA synthesis and RNA function. Over 150 studies of CD-mediated PGT applications have been reported since 2000, all using wild-type enzymes. However, various forms of CD are limited by inefficient turnover of 5FC and/or limited thermostability. In a previous study, we stabilized and extended the half-life of yeast CD (yCD) by repacking of its hydrophobic core at several positions distant from the active site. Here we report that random mutagenesis of residues selected based on alignment with similar enzymes, followed by selection for enhanced sensitization to 5FC, also produces an enzyme variant (yCD-D92E) with elevated T_m values and increased activity half-life. The new mutation is located at the enzyme's dimer interface, indicating that independent mutational pathways can lead to an increase in stability, as well as a more subtle effect on enzyme kinetics. Each independently derived set of mutations significantly improves the enzyme's performance in PGT assays both in cell culture and in animal models.

Keywords: thermostability; prodrug gene therapy; cytosine deaminase; random mutagenesis; structure

Introduction

The pyrimidine salvage pathway enzyme cytosine deaminase (CD; EC 3.5.4.1) is responsible for converting the nucleobase cytosine to uracil and ammonia. This activity is found primarily in microbes,[1] including *Saccharomyces cerevisiae* and *Escherichia coli*, and has arisen at least twice, using completely separate protein folds.[2,3] In addition to cytosine, CD catalyzes the conversion of 5-fluorocytosine (5FC) to the potent chemotherapeutic drug 5-fluorouracil (5FU). Thus, the combination of CD enzyme activity and 5FC as its substrate forms the basis of a potential antitumor gene therapy, where CD plays the role of a 'suicide' gene.[4]

In suicide gene therapy applications, the gene for CD is introduced into cancer cells, followed by systemic administrations of the prodrug 5FC. Following deamination by CD, 5FU is converted by cellular enzymes to 5FdUMP, an irreversible inhibitor of thymidylate synthase. Inhibition of thymidylate synthase blocks thymidine 5′-triphosphate production

*Corresponding author. E-mail address: blackm@mail.wsu.edu.

† T.S.S. and A.M.K. authors contributed equally to this work and share first authorship.

Abbreviations used: PGT, prodrug gene therapy; CD, cytosine deaminase; 5FC, 5-fluorocytosine; yCD, yeast cytosine deaminase; 5FU, 5-fluorouracil; HSVTK, herpes simplex virus thymidine kinase; GCV, ganciclovir; bCD, bacterial CD; yCD-double, A23L/I140L; yCD-triple, A23L/V108I/I140L; PBS, phosphate buffered saline.

and prevents DNA synthesis.[5–7] The CD/5FC system has been used in numerous animal models[8–10] and is currently being evaluated in clinical trials for solid tumors.[11–15] One limitation to this approach is the poor transfection efficiency of current vector delivery systems. Consequently, high 5FC doses must be administered to achieve therapeutic value and are associated with unwanted side effects suggested to be a result of the generation of 5FU by intestinal bacteria.[16]

Key to suicide gene therapy is the phenomenon known as the bystander effect, in which nontransfected neighboring cells are killed through the transfer of antimetabolites from CD-expressing cells in close proximity. A strong bystander effect has been associated with CD and 5FC because 5FU is a small, uncharged molecule capable of nonfacilitated diffusion through cellular membranes.[17–21] Unlike other suicide gene therapy systems, such as herpes simplex virus thymidine kinase (HSVTK) and ganciclovir (GCV), that rely on transfer of metabolites through gap junctions, the CD/5FC bystander effect is not dependent on cell-to-cell contact.[17]

Another advantage of the CD/5FC combination is that 5FU has radiosensitizing properties.[22,23] Since it is unlikely that treatment with gene therapy would be the only course of action in patients, radiosensitizing effects can augment treatment regimens. Several groups have reported *in vivo* results with CD to have a significant bystander effect[22,24] at clinically relevant 5FC doses and radiation regimens.[8,22,25]

Two completely separate forms of CD have evolved in nature, and both are being studied in antitumor gene therapy investigations. Yeast CD (yCD) belongs to the amidohydrolase protein fold family (CATH topology class 3.40.140) and shares homology with bacterial and eukaryotic cytidine deaminases.[3] The enzyme is assembled into a homodimer composed of 17.5-kDa subunits that contain a catalytic zinc ion. In contrast, bacterial CD (bCD) belongs to the α/β 'TIM' barrel fold family (CATH topology class 2.30.40) and most closely resembles human adenosine deaminase.[2] In *E. coli*, the enzyme is assembled into a hexamer of 60-kDa subunits that contain a catalytic iron.

Although product release from the yCD is rate limiting,[26] yCD has been observed to display superior kinetic properties toward 5FC (corresponding to a 22-fold lower K_m for the prodrug) and slightly improved efficacy for treating tumors in mice than bCD.[27] However, wild-type yCD is relatively thermolabile as compared with bCD,[27,28] a property that may limit its performance in therapeutic applications.

Using computational protein engineering, we previously created a series of mutant yCD variants that display elevated unfolding temperatures in denaturation experiments and increased half-lives of catalytic activity at elevated temperatures.[29] An enzyme mutant with two substitutions (A23L/I140L or 'yCD-double') and a subsequent, final redesigned mutant (A23L/V108I/I140L or 'yCD-triple') display wild-type catalytic efficiencies and 5- and 30-fold increases in the half-lives of those catalytic activities. Furthermore, yCD-double and yCD-triple display apparent melting temperatures 6 and 10 °C greater, respectively, than wild-type yCD. The latter construct also displayed improved complementation of CD activity at elevated temperatures in bacteria.

In the present study, we have randomly mutagenized residues that were selected based on sequence conservation with similar enzymes and have used positive and negative genetic complementation strategies to identity mutations that confer increased 5FC sensitivity (i.e., those that lead to toxicity at the lowest possible concentrations of 5FC). The resulting mutations were analyzed alone and in combination with those previously engineered in the protein core for their effect on (1) prodrug sensitivity in mammalian cells and in a mouse xenograft tumor model, (2) substrate specificity, (3) kinetic efficiency, and (4) thermal unfolding of the enzyme and the half-life of catalytic activity. The crystal structure of the mutant from the screen that induced the most significant increase in 5FC sensitivity was determined. The computationally engineered yCD-triple and the genetically selected yCD-D92E variant each separately provides enhanced 5FC sensitivity to cells and therefore may serve as improved candidates for future suicide gene therapy studies. In contrast, the combination of these mutations abrogates their individual contribution to improved performance in prodrug gene therapy (PGT) assays, possibly due to the accumulation of individual small reductions in catalytic efficiencies that reach a critical threshold for sensitization to 5FC.

Results

Identification of mutants in and near the active site that confer enhanced 5FC sensitivity

To create yCD variants with increased activity to 5FC, we subjected 11 codons within the most conserved region of yCD (T83, L84, Y85, T86, L88, S89, D92, M93, T95, G96, and I98) to regiospecific, partially randomizing mutagenesis as described in Materials and Methods. Absolutely conserved residues within this same region, assumed to be critical for activity, were omitted from randomization (T87, P90, C91, and C94). Fig. 1 shows a model of two views of yCD (purple residues indicate the locations of the triple-amino-acid substitutions A23L/V108I/I140L), with targeted residues highlighted in blue.

Identification of functional yCD variants with enhanced 5FC activity involved a two-step selection procedure. First, functional yCD variants were selected for preservation of catalytic activity, based on their ability to confer growth on cytosine-containing plates, under conditions that require CD activity for viability. Second, the functional variants were then screened on cytosine plates containing 5FC. It was determined that the 5FC dose at which wild-

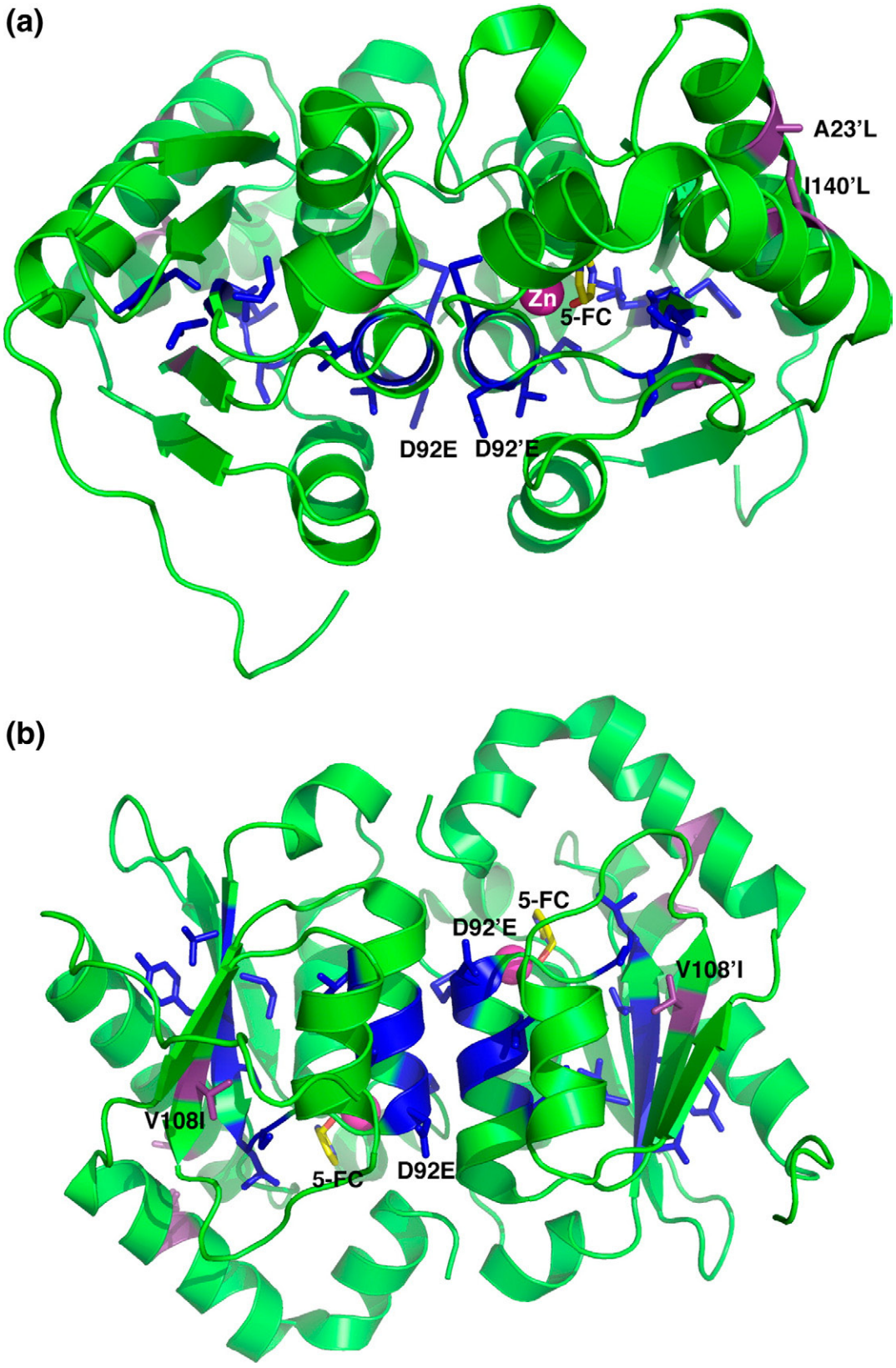

Fig. 1. Ribbon diagram of the yCD homodimer [side view in (a) and bottom view in (b)] showing the location of 11 residues that were subjected to randomization and subsequent selection for 5FC sensitization (side chains shown as blue sticks) and 3 residues that were previously redesigned to increase packing between structural elements and thus increase thermostability (shown in purple). The location and nature of mutations characterized in this article (D92E from selection; A23L, V108I, and I140L) are labeled. Each mutation is found once in each protein subunit.

type yCD survives, or the sublethal dose, is 77.45 μM. Although wild-type pETHT:yCD will allow growth on plates containing the sublethal dose of 5FC, any mutant with increased 5FC activity will not be viable. Colonies were sequentially streaked onto plates containing 5FC from 77.45 to 3.87 μM to identify the best variants within the library pool. From an estimated total of 34,000 transformants, 50 colonies (~0.15%) were identified as yCD positive based on their ability to grow on cytosine-containing plates. Of the 50 yCD-positive clones, only 6 conferred sensitivity at 3.87 μM 5FC, the lowest effective 5FC concentration in the negative selection.

Plasmid DNA from colonies on the nonselective and selective plates was isolated and sequenced in order to evaluate the library diversity, along with identifying which substitutions are tolerated. Sequence analysis of DNA isolated from colonies that grew on the nonselected plates revealed a broad spectrum of mutations in the regiospecific library (data not shown) and indicates that the oligonucleotides used to generate the library contained random sequences. Sequence analysis of the six variants that conferred the greatest sensitivity to *E. coli* revealed that two had a substitution at D92 to glutamic acid (D92E), two had a substitution at M93 to leucine (M93L), and two had a substitution of I98 to leucine (I98L). Additionally, the two I98L mutants have different nucleotide-level changes, suggesting that these mutants were derived independently. Therefore, from a library of 34,000 transformants, three amino acid substitutions that confer 5FC sensitivity (D92E, M93L, and I98L) at the lowest 5FC concentration in the selection scheme were identified.

Construction of combinations of yCD mutants

Recently, we performed a computational design study aimed at improving the stability of the thermolabile yCD,[29] in which mutations were generated in the enzyme's hydrophobic core, distant from the active site. Several new mutants were constructed by site-directed mutagenesis to investigate the combined effects of these mutations with those selected from the mutagenesis study as described above. These 'superimposed' mutants (yCD-triple/D92E, yCD-triple/M93L, and yCD-triple/I98L) and their individual parental mutations were then tested in a mammalian tumor cell line assay for increased 5FC sensitivity.

In vitro 5FC sensitivity assays

Mammalian expression vectors encoding the yCD variants were constructed and used to transfect rat C6 glioma cells (see Materials and Methods) to determine the activity of these mutants toward 5FC (and their ability to induce sensitivity to 5FC) *in vitro*. Immunoblot analyses of lysates from the pools of transfectants show similar yCD expression levels for all of the mutants and wild-type yCD, with no detectable expression in vector control pools (data not shown). Pools of stable transfectants were assayed for 5FC sensitivity over a drug range of 1–10 mM. Representative results of the 5FC sensitivities displayed by the yCD mutants, wild-type yCD, and a vector control are shown in Fig. 2. Little to no toxicity was observed with vector alone at the lower 5FC doses; however, above 6 mM 5FC, an inherent cytotoxicity is observable in the glioma cell line. yCD-D92E displays the greatest reduction in IC_{50} (~30%) for 5FC of the three regiospecific random mutants (Fig. 2a). No difference in sensitivity was observed with the yCD-I98L substitution as compared with wild-type yCD. The yCD-M93L mutant displays an intermediate IC_{50} of 9.5 mM, an estimated decrease of 15% from wild-type yCD.

The computationally designed thermostabilizing yCD-double and yCD-triple mutants also display increased sensitivity toward 5FC in glioma cells (Fig. 2b). The yCD-double mutant displays an IC_{50} (8 mM) similar to that of yCD-D92E, an approximate 30% reduction in IC_{50} compared with wild-type yCD-transfected cells. The greatest enhancement in activity was observed with the yCD-triple mutant, with an IC_{50} of approximately 6 mM, an estimated 50% reduction relative to wild-type yCD.

Unexpectedly, none of the superimposed mutants exhibits enhanced activities toward 5FC. The yCD-triple/I98L and yCD-triple/M93L have an IC_{50} of 9 mM (data not shown), while the yCD-triple/D92E has an IC_{50} similar to that of wild-type yCD-transfected cells (Fig. 2c). These results indicate that the addition of the randomly generated substitutions to the designed mutant negates the effect introduced by the triple substitutions.

5FC sensitivity assayed using a xenograft tumor model

The behaviors of the two most active yCD constructs from the assays above (yCD-triple and yCD-D92E) were then further compared with those of wild-type enzyme and a negative control in a mouse xenograft model of PGT. As described in Materials and Methods, pools of rat C6 cells stably transfected with pCDNA containing yCD, yCD-triple, yCD-D92E, or vector alone (0.5×10^6 cells) were subcutaneously injected into the flanks of nude mice ($n = 5$). When the tumor size reached 3–4 mm, phosphate buffered saline (PBS) or 5FC at 500 mg/kg was injected intraperitoneally once a day for 18 days. Tumor size was monitored every other day. Tumor cells transfected with vector only (pCDNA) showed no statistical difference in tumor size between mice treated with PBS and those treated with prodrug (Fig. 3a). Similarly, no statistical difference was observed in tumor volume in mice seeded with cells transfected with pCDNA:yCD that were injected with PBS or 5FC (Fig. 3b). The lack of difference in wild-type yCD tumor size between PBS- and 5FC-treated mice on day 18 is likely a reflection of the low 5FC dose administered and/or the duration of the prodrug treatment.

In contrast to tumors expressing wild-type yCD, the prodrug-treated mice bearing yCD-triple- or

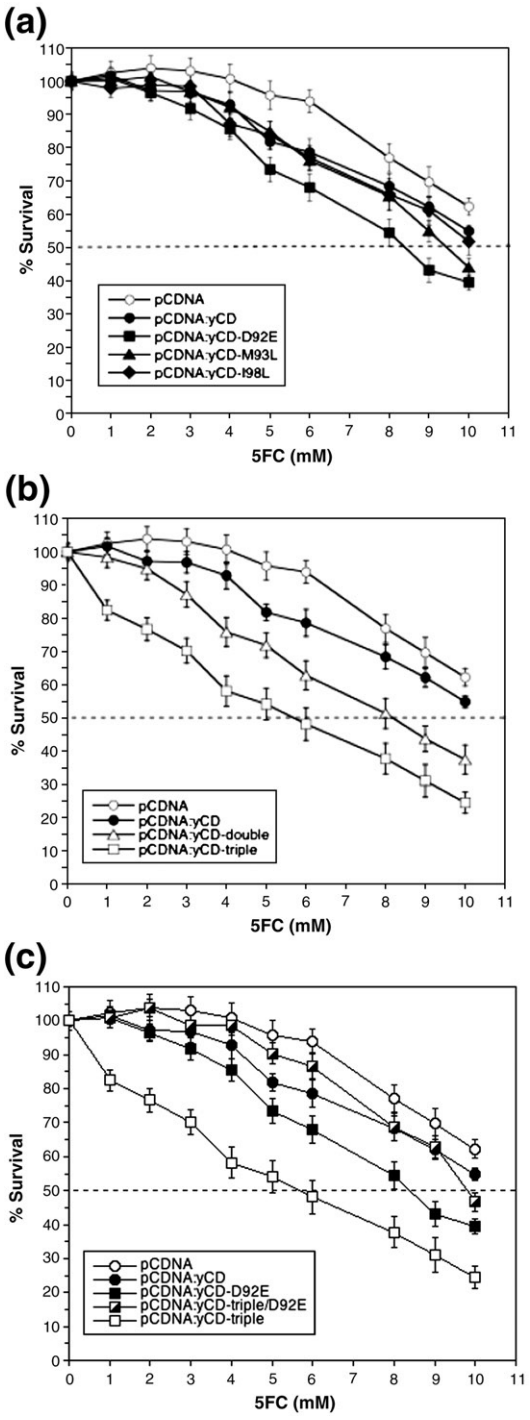

Fig. 2. Sensitivity of selected, computationally designed, or superimposed mutant yCD-expressing rat C6 glioma transfectants to 5FC. Pools of stable transfectants containing vector only (pCDNA), wild-type yCD, (a) regiospecific random mutants (D92E, M93L, or I98L), (b) computationally designed thermostable mutants (double and triple), or (c) the superimposed mutant (yCD-triple/D92E) were used to transfect rat C6 glioma cells and evaluated for 5FC sensitivity as described in Materials and Methods. After 6 days of 5FC treatment, cell survival was determined using Alamar Blue according to the manufacturer's instructions. Each data point (mean±SEM; $n=3$; performed with at least 15 replicates) is expressed as a percentage of the value for control wells with no 5FC treatment.

yCD-D92E-expressing tumors elicited a strong response (Fig. 3c and d). The mice bearing yCD-triple-expressing tumors treated with 5FC displayed the greatest restriction in tumor growth (mean tumor volume of 1076 mm^3 *versus* PBS tumor mean of 2833 mm^3; $P=0.05$). The yCD-D92E tumor-bearing mice also showed restricted growth in the presence of 5FC (733 *versus* 1942 mm^3 for saline-treated mice; $P=0.035$). The mean tumor size of the prodrug-treated group was divided by the mean tumor size of the prodrug-treated group for each group on day 18 to compare the effects of 5FC on tumors expressing the redesigned thermostabilized yCD-triple with those of the selected yCD-D92E. Both yCD-triple tumor-bearing mice and yCD-D92E tumor-bearing mice responded equally well (2.65 *versus* 2.64, respectively).

Enzyme kinetics and thermostability

The unexpected loss of *in vitro* sensitivity toward 5FC when yCD-triple and yCD-D92E were combined, as compared with their individual behaviors, led us to investigate the catalytic and biophysical properties of these yCD variants in more detail. Using purified proteins, we performed enzyme assays with cytosine and 5FC as substrates as described in Materials and Methods.

Overall, the relative catalytic efficiency (k_{cat}/K_m) toward cytosine of the individual yCD-triple or yCD-D92E mutants is not appreciably different from that of wild-type enzyme, whereas the yCD-triple/D92E is approximately 3-fold less efficient (Table 1). This result is primarily caused by a reduction in the enzyme's turnover rate: k_{cat} (cytosine) for yCD-triple/D92E is approximately one-eighth that of wild-type enzyme. In contrast, the K_m values for cytosine observed with all mutant enzymes are all within approximately 2- to 2.5-fold of wild-type yCD values (Table 1).

When the prodrug 5FC is instead used as the substrate in kinetic assays, the individual yCD-triple and yCD-D92E mutant enzymes again display overall catalytic efficiencies (k_{cat}/K_m) that are roughly equivalent to wild-type yCD (Table 1). This corresponds to slightly higher K_m values (1.7- and 1.8-fold, respectively) balanced by small increases in k_{cat}. In contrast, although the combined yCD-triple/D92E enzyme has a slightly lower K_m, it displays a k_{cat} value half that of wild-type yCD. This gives the combined yCD-triple/D92E mutant enzyme a slightly impaired 5FC catalytic efficiency (1.6-fold) compared with wild-type yCD, yCD-triple, and yCD-D92E.

Inside a cell, cytosine and 5FC compete for the active site of yCD. To take this into account, the relative specificities or substrate preference for 5FC of all three mutant enzymes was compared (calculated as $[k_{cat}/K_{m\ (5FC)}/(k_{cat}/K_{m\ (5FC)}+k_{cat}/K_{m\ (cyt)})]$). With wild-type yCD set at a relative specificity of 1.0, there is no significant difference in substrate preference between yCD-wild type (1), yCD-triple (0.947), and yCD-D92E (1.12) and only a modest 1.23-fold increase in preference for 5FC displayed by

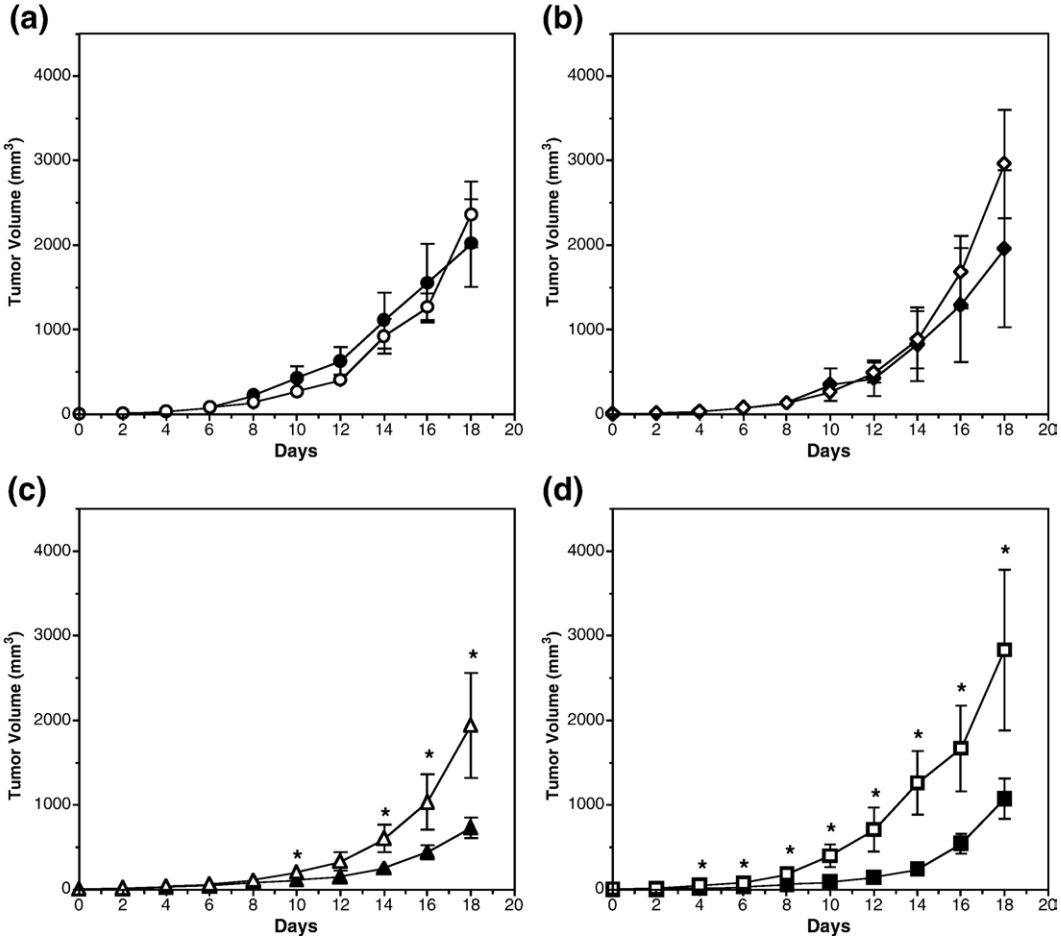

Fig. 3. Growth of tumors expressing yCD during 5FC treatment. Pools of rat C6 glioma cells transfected with (a) vector, (b) wild-type yCD, (c) yCD-triple, or (d) yCD-D92E were used to seed tumors in nude mice. When tumor size reached 3–4 mm (day 0), PBS (open symbols) or 5FC (500 mg/kg, closed symbols) was administered once a day for 18 days. During this period, tumor growth was measured every other day ($n=5$ for each group). Tumor volume was calculated using the formula $4/3\pi((\text{Width}\times\text{Length}\times\text{Height})/2)$, plotted, and analyzed for statistical significance using Student's t test. Asterisks denote statistical significance ($P\leq 0.05$).

the yCD-triple/D92E mutant. This modest shift in specificity toward 5FC for the combined mutant is not correlated with what was observed in cell sensitivity assays, where yCD-triple/D92E performed no better than the wild-type enzyme.

In previous experiments we showed that the redesigned yCD-double and yCD-triple mutants display unfolding temperatures (T_m) in circular dichroism experiments that are 6 and 10 °C higher, respectively, than those of the wild-type enzyme (wild-type yCD, $T_m=52$ °C; yCD-double and yCD-triple mutants, $T_m=58$ °C and $T_m=62$ °C, respectively).[29] The stabilization of yCD in the yCD-triple mutant corresponds to improved complementation

Table 1. Enzyme kinetics

	K_m (mM substrate)	V_{max} (M prod/s)	k_{cat} (M prod/s M E)	k_{cat}/K_m (1/s M E)
Substrate: 5FC				
yCD-wild type	0.083	1.87E−05	18.8	2.26E+05
yCD-triple	0.14	2.95E−05	29.5	2.09E+05
yCD-D92E	0.15	3.17E−05	31.7	2.16E+05
yCD-triple/D92E	0.068	9.51E−06	9.5	1.39E+05
Substrate: Cytosine				
yCD-wild type	1.17	1.70E−04	170	1.45E+05
yCD-triple	0.57	8.62E−05	86.2	1.53E+05
yCD-D92E	0.52	5.18E−05	51.8	1.00E+05
yCD-triple/D92E	0.47	6.53E−05	21.8	4.59E+04

M, molar; E, enzyme.

of CD activity in *E. coli* at elevated temperatures[29] and presumably is also responsible for its improved performance in PGT assays in this study.

We therefore examined the effects of the individual yCD-D92E substitution and of the superimposed yCD-triple/D92E mutation on protein stability. Thermal unfolding experiments were performed on the wild-type, yCD-triple, yCD-D92E, and yCD-triple/D92E proteins using circular dichroism spectroscopy as outlined in Materials and Methods (see also Fig. 4). Although the yCD-D92E mutant was selected based on its ability to confer increased sensitivity to 5FC in *E. coli*, this enzyme unexpectedly also displays an increase in its apparent denaturation temperature, corresponding to a T_m 4 °C higher than the T_m for wild-type yCD. Combination of yCD-D92E with the previous yCD-triple mutations in the enzyme core results in a dramatic 16 °C increase in apparent T_m as compared with wild-type yCD (6 °C higher than that of the yCD-triple mutant). For all of the enzyme constructs, thermal unfolding was irreversible, presumably due to aggregation. Similar to previous studies of the computationally repacked yCD variants,[29] the half-life of the enzyme activity for yCD-D92E and that for yCD-triple/D92E are increased relative to their wild-type and yCD-triple parents, respectively (data not shown).

Table 2. Data collection and refinement statistics

	yCD-triple/D92E bound to dihydropyrimidine
Data collection	
Space group	$P2_12_12_1$
Cell dimensions (Å)	55.9, 69.1, 74.2
Resolution (Å)	2.30 (2.38–2.30)
R_{merge}	0.042 (0.087)
I/σ_I	8.5 (7.5)
Completeness (%)	99.2 (98.8)
Redundancy	7.2 (7.3)
Total reflections	96,421
Unique reflections	13,334
Refinement	
Resolution (Å)	2.30
No. of reflections	13,204
R_{work}/R_{free}	0.204/0.258
No. of atoms	2548
Protein	2396
Ligand/ion	19
Water	133
B-factors	18.1
Protein	17.9
Ligand/ion	11.3
Water	24.2
r.m.s.d.	
Bond lengths (Å)	0.006
Bond angles (°)	1.10
Ramachandran distribution (% core, allowed, disallowed)	98.7, 1.0, 0.3

Values in parentheses are for the highest-resolution shell.

Structure determination

The crystal structure of yCD-triple/D92E bound to a transition state analog was solved at 2.3-Å resolution (Table 2) and compared with both previously solved wild-type [Protein Data Bank (PDB) accession code 1p6o] and triple-mutant (PDB accession code 1ysb) structures in order to identify any potential structural changes that may explain the observed IC_{50} values as well as the thermodynamic and kinetic data. The yCD-D92E and yCD-triple mutations appear far from the active site (Fig. 5a), and indeed the active site residues show no perturbation when either the yCD-triple or yCD-D92E/triple structure is compared with wild-type enzyme (Fig. 5b). The yCD-D92E mutation, although close in sequence to active site residues C91 and C94, is actually involved in the dimer interface of the homodimeric enzyme. In the wild-type enzyme, both carboxyl oxygens in aspartate 92 make a salt-bridge contact to a nearby arginine residue in the adjacent monomer (Fig. 6a), with oxygen-to-nitrogen distances of 3–3.5 Å. In yCD-D92E, the extra carbon in the glutamate is packed against a nearby lysine and isoleucine, resulting in a redistribution of contacts made by the carboxylate oxygens of the mutated side chain (Fig. 6b). In this

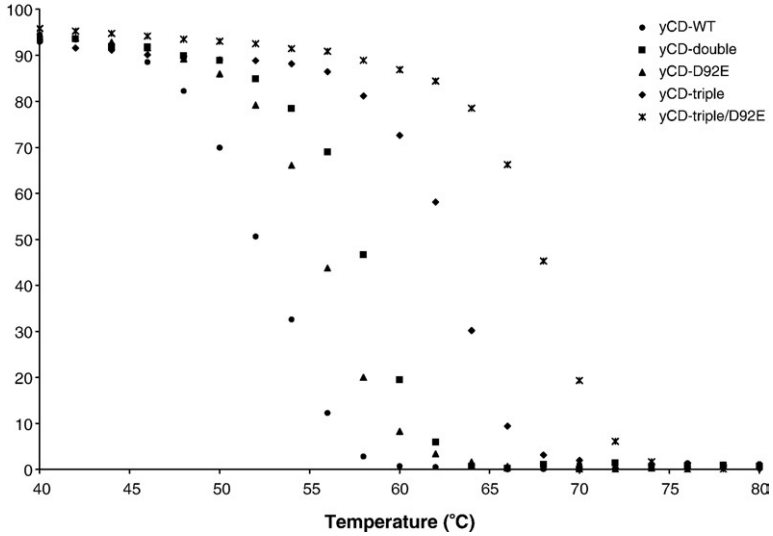

Fig. 4. Thermal denaturation measurements of the wild-type and variant yCDs. The temperature melt measures the change in signal at 220 nm over a range of temperatures (°C). All constructs show a folded baseline followed by a sigmoidal two-state transition to an unfolded baseline. The baseline plateaus correspond to an assignment of 100% folded protein.

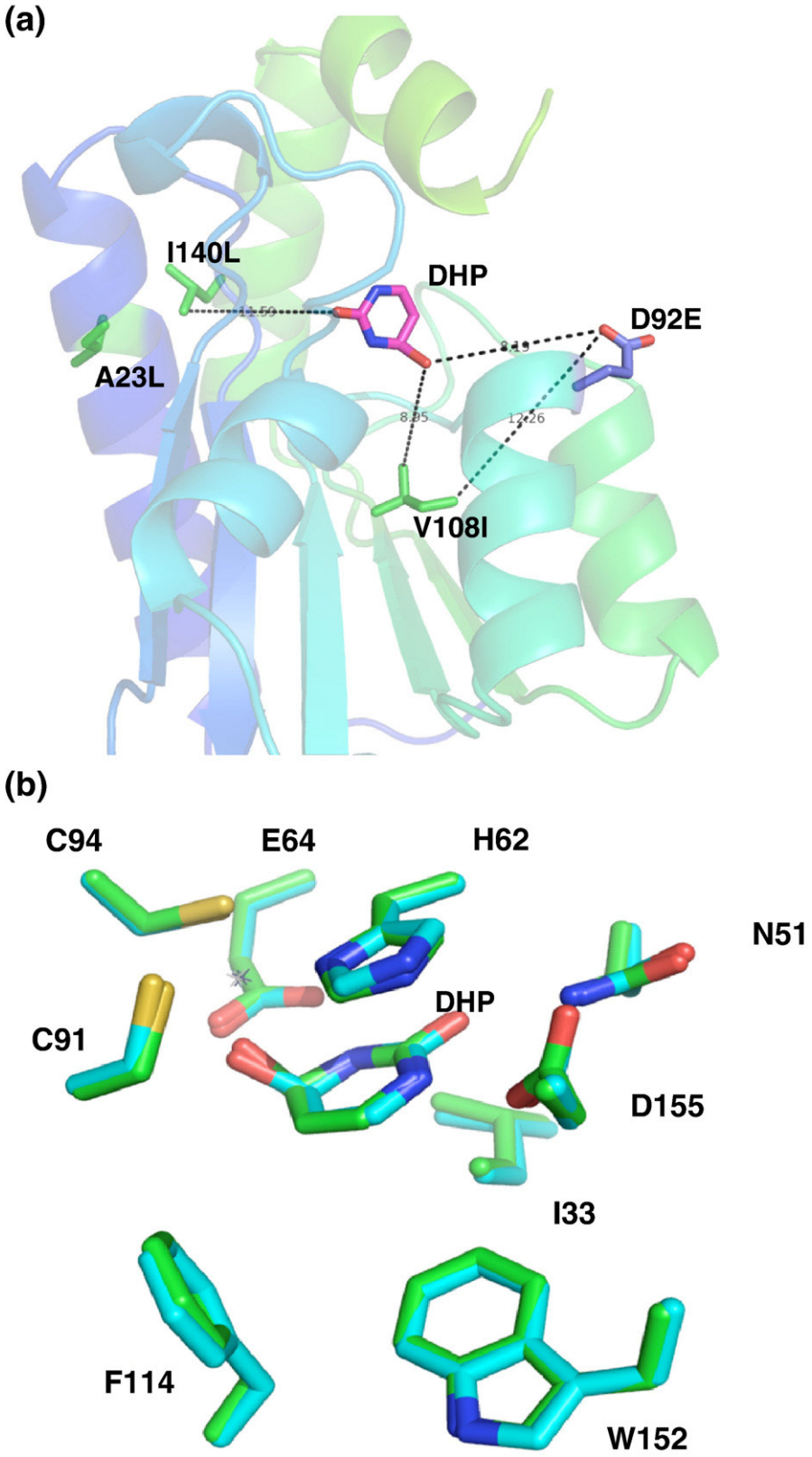

Fig. 5. Crystal structure analysis of the yCD-triple/D92E active site. (a) Location and relative distances of mutated residues from a mechanism-based inhibitor (dihydropyrimidine or DHP) that acts as a mimic of the reaction transition state. All residue atoms are located over 8 Å from the substrate analog, including the residue (D92E) selected in a screen for 5FC sensitization. (b) Superimposition of wild-type and yCD-triple/D92E active site residues.

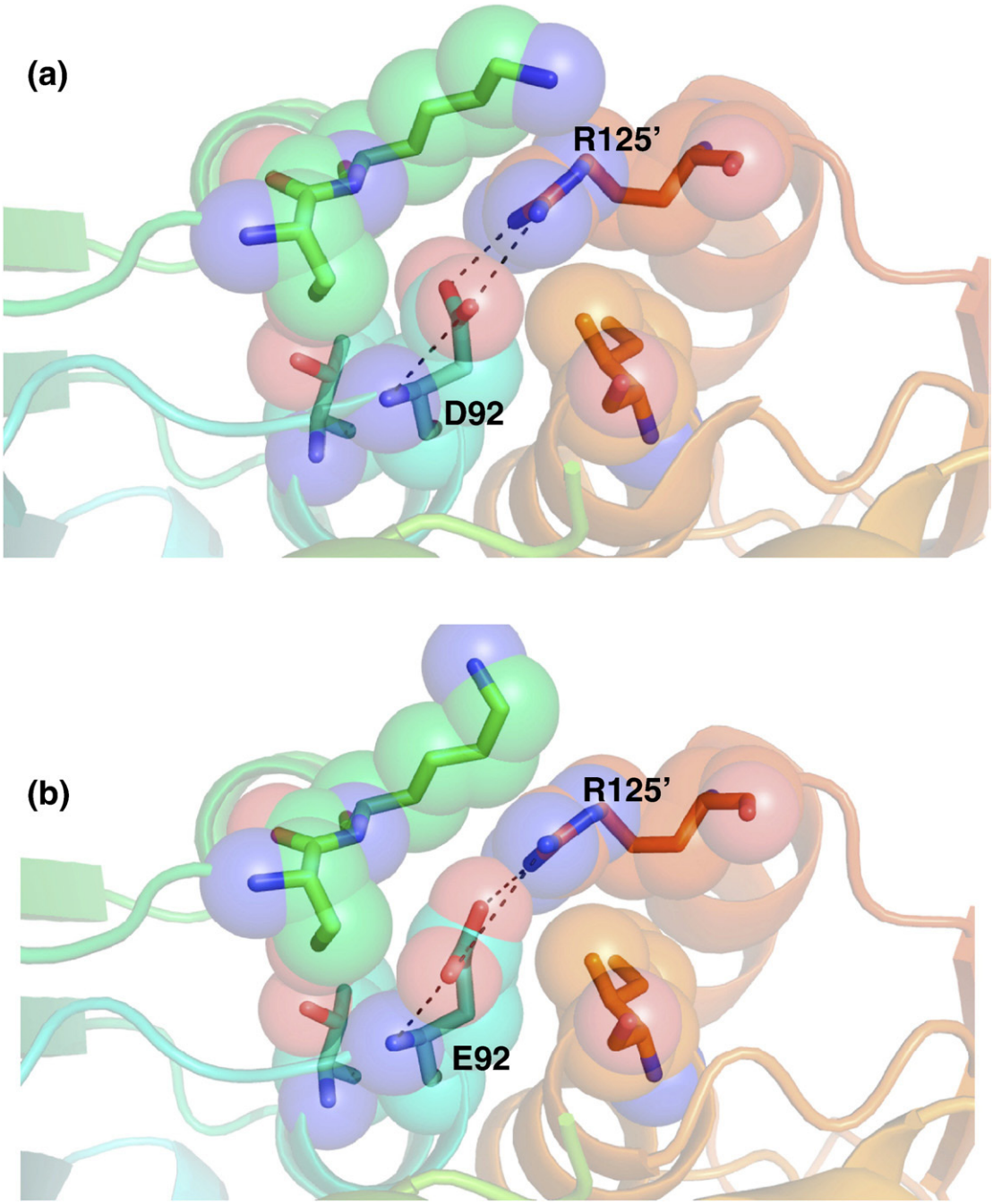

Fig. 6. Interaction and position of (a) wild-type D92 at the dimer interface and (b) mutant E92 at the dimer interface with its surrounding neighbors. The mutation causes a very small rearrangement of the side chain torsion angles and interactions between the mutated residue and its nearest neighbor, R125. No other significant structural perturbation due to D92E is apparent.

structure, one oxygen-to-nitrogen distance is considerably shorter (~2 Å), while the second is lengthened.

Discussion

The initial premise of this study was that independent mutations near the active site and within the hydrophobic core of yCD, which respectively influence substrate specificity and enzyme thermostability, could each be identified in separate experiments and then combined in a single construct for maximum benefit. Furthermore, whereas stabilizing interactions in a protein core can be improved through computational protein design,[29] an enzyme's substrate specificity is still more effectively addressed through incorporation of random mutations and subsequent genetic screens or directed evolution protocols. Thus, a two-pronged experimental approach to improve the physical and catalytic properties of yCD was expected to yield a

combination of enzyme mutations with optimal properties.

Instead, the experiments described above yielded unexpected results in three ways. First, the protocol of random mutagenesis and genetic screening generated a construct (yCD-D92E) that displayed an increase in its unfolding temperature T_m, in addition to a small (1.12-fold) specificity shift toward 5FC relative to cytosine. This result appears to have been made possible through the choice of residues that were subjected to mutation, which extended beyond the substrate binding pocket to nearby positions involved in dimerization. Residues were chosen for mutation prior to determination of the enzyme's structure, based on sequence conservation across the closest known homologs with deaminase function. In retrospect, strongly conserved residues in yCD (and most other enzymes) include not only those positions most critically involved in substrate recognition and catalysis but also amino acids that closely couple the architecture of the active site to the fold and stability of the enzyme tertiary structure (e.g., D92).

Second, the stabilized mutant yCD constructs produced by repacking of the hydrophobic core (yCD-double and yCD-triple) were significantly improved in their performance in PGT assays, with the latter construct actually outperforming the best mutant construct selected solely on the basis of 5FC sensitivity. This result, considered in concert with the properties of yCD-D92E described above (improved stability and nominal changes in catalytic behavior), may indicate that the primary limiting behavior of wild-type yCD for PGT is its stability, which presumably is coupled to steady-state enzyme levels in transfected cells and enhanced conversion of 5FC to 5FU.

Finally, the combination of two sets of physically separate mutations (yCD-triple and yCD-D92E) that were independently generated failed to act in a synergistic or additive manner in PGT assays when combined into a single construct. On the surface, an explanation for this behavior seems straightforward: the combined construct (yCD-triple/D92E) is significantly more thermostable than any of the individual yCD constructs (with an apparent increase in T_m of 16 °C), which might lead to a corresponding reduction in catalytic efficiency at physiological temperatures due to reduced conformational dynamic flexibility of the protein backbone. However, the difference in kinetic rate and catalytic efficiency toward 5FC exhibited by yCD-triple or yCD-D92E compared with yCD-triple/D92E (which performs similarly to wild-type enzyme) is not dramatic: the combined mutant is perhaps 1.5-fold less active toward the prodrug than the individual mutants. This result might imply that there exists a quite sharp 'threshold' of activity toward 5FC deamination in the cell that leads to considerably more sensitivity toward low concentrations of the prodrug. For this to be true, the specific activity of the wild-type enzyme under standard protocols of transfection and expression would have to be somewhat close to that critical point of metabolic sensitivity. However, alternative situations might also explain the poor performance of the combined mutations in PGT assays, including (but not limited to) unexpectedly reduced expression levels in eukaryotic cells, abnormal protein localization, trafficking, or protein turnover or unexpected effects on kinetic specificity and activity (e.g., inhibition in cells by a nucleobase analog that is not accounted for in these studies).

Variable routes to protein thermostabilization

Two entirely separate forms of thermostabilized yCD enzymes have been generated in these studies, one of which was generated in a screen for increased sensitivity to 5FC and the other in a structure-based redesign protocol intended to produce a more robust form of the enzyme. The independent sequence changes that lead to stabilization (increased van der Waals packing of each subunit's hydrophobic core *versus* more subtle alteration of contacts in the homodimer interface) are structurally dissimilar from one another, providing a clear demonstration that multiple evolutionary routes can act on protein stability through considerably different structural mechanisms.

This result reinforces a myriad of studies of protein stability conducted over the past 10 years, where the structures of homologous proteins from various biological sources (ranging from cryophiles to mesophiles to thermophiles) have been directly compared in attempts to catalog the determinants of protein stability.[30–35] Although a variety of factors have been implicated in thermostability (including hydrophobic packing, formation of additional salt bridges within the protein structure, modifications of surface charge distribution, and shifts in amino acid composition, to name just a few), each mechanism appears to be relatively unique to specific structural families of proteins. In addition, individual proteins can be made thermostable either by reducing their relative free energy in the folded state (termed 'thermodynamic stabilization') or by decreasing the rate of unfolding through modifications that increase the energy barrier of the unfolding transition state (termed 'kinetic stabilization'). The latter mechanism for protein stabilization has been observed for a variety of proteins, such as α-lytic protease.[36] A significant aspect of such proteins is the identification of residues at points distant from the hydrophobic core and often at domain interfaces, which are highly sensitive to mutational effects on protein stability.[37] Given the nature of the yCD-D92E mutation at the dimer interface, which does not appear to obviously increase favorable contacts in the folded enzyme, it might be possible that this mutation stabilizes yCD via this latter mechanism.

yCD and 5FC and enzyme engineering in recent gene therapy trials and the role of optimized enzyme constructs

Between 1990 and 2004, 405 gene therapy trials were approved in the United States for cancer

treatment, 95 of which contain various elements of enzyme/prodrug therapeutic strategies;[38] 78 of these trials were active as of July 2007‡. Three of these trials, all involving the combination of HSVTK and GCV, have advanced to phase III multicenter programs.[38,39] A large percentage of these trials have targeted prostate cancer, due to the relatively low percentage of these cancers that have associated detectable metastatic disease (<10%) at the time of diagnosis.[11] Of these latter trials, many have made use of CD enzymes and 5FC, most in combination with additional enzyme/prodrug activities.[11–15] Results from phase I trials against prostate cancer and pancreatic cancer have recently been reported for combined PGT therapies involving yCD. In each study, a replication-competent adenovirus armed with wild-type yCD fused to a modified HSVTK (SR39), in combination with 5FC/GCV prodrug administration and radiation, was utilized.[11] In both cases, the trimodal approach (oncolytic virus, suicide gene/prodrug, and radiation) significantly increased tumor control beyond that displayed by individual modalities, with a corresponding reduction in morbidity and toxicity as compared with traditional chemotherapy. As well, positron emission tomography studies indicated strict localization of the transfected gene and its product in the targeted tissue.

Despite the promise of such studies, PGT is limited pharmacokinetically by the ability to deliver the suicide gene efficiently to tumor cells, whereas traditional chemotherapeutic strategies are perhaps equally limited by the ability to specifically target the effects of cytotoxic agents to tumor cells at levels over normal proliferating cell populations in the body. The ability of PGT to effectively ablate tumor cells is also reliant on the inherent sensitivity that cell type displays toward a particular gene/prodrug combination. Additionally, when poor responsiveness necessitates repeat therapeutic intervention, rapid immune clearance of cells expressing a previously seen foreign protein may serve to further limit treatment efficacy. As such, various enzyme/prodrug combinations will be required to accommodate these various treatment scenarios. The pharmacokinetic properties of the enzyme (its stability, half-life, and kinetic activity), the prodrug (its metabolism and toxicity), and the combination of the two (their uniqueness to transfected cells) must be optimized for maximum therapeutic efficacy to offset the significant hurdles associated with PGT. In particular, the catalytic efficiency of enzymatic activation of the prodrug and the relative level of activation of the prodrug in transfected cells must be optimized for several enzyme/prodrug combinations. For the most commonly used enzyme/prodrug combination under clinical study to date (HSVTK and GCV), random mutagenesis and genetic selection experiments have generated a variant of HSVTK (SR39) that has led to a 294-fold increase in sensitivity to GCV when compared with wild-type enzyme, as well as improved tumor growth inhibition.[40,41]

In the case of CD and 5FC, the availability of two separate enzyme scaffolds and folds (yCD and bCD) further increases the parameters that can be optimized and combined with other enzymes; each enzyme displays unique characteristics of size, oligomeric structure, behavior when 'tethered' to additional enzymes, metal dependence, stability, and substrate specificity profiles. Given that a variety of studies that use two enzyme/prodrug combinations have shown synergistic improvements in efficacy over individual enzyme systems,[42–45] the utility of kinetic and biophysical optimization of each enzyme seems clear. Thus, side-by-side optimization of each enzyme source for PGT is likely to illuminate the balance of properties that are most critical for performance in gene therapy applications.

Materials and Methods

Materials

Oligonucleotides used to mutate and sequence yCD were obtained from either Sigma-Proligo (St. Louis, MO) or Integrated DNA Technologies (Coralville, IA). Restriction enzymes were obtained from New England Biolabs (Beverly, MA). The plasmid pETHT:yCD expressing His-tagged yCD was constructed as described by Ireton *et al.*[3] DNA purification was done using several kits: Wizard PCR prep kits from Promega (Madison, WI), HiSpeed Plasmid Mini Kit from Qiagen (Valencia, CA), and StrataPrep EF Plasmid Midikit from Stratagene (La Jolla, CA). Alamar Blue was purchased from Serotec Limited (Oxford, UK). All cell culture reagents were purchased from Gibco (Carlsbad, CA). All other reagents were purchased from Sigma (St. Louis, MO) unless otherwise noted.

Bacterial strains

E. coli GIA39, a strain deficient in CD and orotidine 5′-phosphate decarboxylase, was obtained from the *E. coli* Genetic Stock Center (CGSC no. 5594: *thr*$^-$ *dad*B3 *fhu*A21 *cod*A1 *lac*Y1 *tsk*-95 *gln*V44(AS) λ^-*pyr*F101 *his*-108 *arg*G6 *ilv*A634 *thi*-1 *deo*C1 *glt*-15). *E. coli* GIA39 was lysogenized with DE3 according to the manufacturer's instructions (Novagen, Madison, WI). The derived strain, GIA39(DE3), was used in the genetic complementation assays for CD activity. *E. coli* strain CJ236 (F^+LAM$^-$, *ung*-1, *rel*A1, *dut*-1, *spo*T1, *thi*-1) was used to produce single-stranded DNA for site-directed mutagenesis procedures. The *E. coli* strain NM522 [F^+ *lacI*^{q} Δ(*lacZ*)-M15 *pro*A$^+$B$^+$/*sup*E *thi*Δ(*lac–pro*AB) Δ(*hsd*MS–*mcr*B)5($r_k^-m_k^-$McrBC$^-$)] and *E. coli* strain XL1-Blue [F′: :Tn10 *proA*$^+$*B*$^+$ *lacI*^{q} D(*lacZ*) *M15/recA1 endA1 gyrA*96 (Nal^r) *thi hsdR17* ($r_K^-m_K^+$) *supE44 relA1 lac*] were used as recipients for certain cloning procedures. *E. coli* BL21-RIL (Novagen, Madison, WI) was used for large-scale protein purification.

Construction of the yCD regiospecific random library

Preparation of the randomized insert

The basic protocol for regiospecific random mutagenesis was performed as outlined by Kurtz and Black.[46]

‡ http://www.wiley.co.uk/genetherapy/clinical/

Table 3 lists the oligonucleotides MB223–MB236 designed to synthesize a 139-bp double-stranded DNA fragment that spans 11 codons (T83, L84, Y85, T86, L88, S89, D92, M93, T95, G96, and I98) and contains 21% randomness at those positions.

Briefly, the 139-bp double-stranded DNA fragment was synthesized by annealing 50 pmol each of MB223 and MB224 with 10× annealing buffer (70 mM Tris–HCl, pH 7.5, 60 mM $MgCl_2$, and 200 mM NaCl) in a final volume of 50 μL at 95 °C for 5 min, at 65 °C for 20 min, and at room temperature for 10 min. Next, the annealed product was extended with the Klenow fragment of *E. coli* DNA polymerase in an 80 μL reaction mixture consisting of the 40 μL annealed product, 4 μL 10× annealing buffer, 5.6 μL 10 mM deoxyribonucleotide triphosphates, 1.6 μL 0.1 M DTT, and 4.8 μL Klenow fragment (5 U/μL) at 37 °C for 30 min, at 65 °C for 10 min, and at room temperature for 10 min.

Amplification of the random insert

A master mix was prepared consisting of 110 μL of 10× PCR buffer (200 mM Tris–HCl, pH 8.3, 250 mM KCl, 15 mM $MgCl_2$, and 0.5% Tween-20), 200 pmol each of MB225 and MB226, 4.4 μL of 10 mg/mL bovine serum albumin, 5.5 μL of 10 mM deoxyribonucleotide triphosphates, and 4.4 μL of *Taq* polymerase (5 U/μL). The extended product (16 pmol or 5 μL) and 27.8 μL of the master mix were mixed to a final volume of 200 μL and split into four tubes containing 50 μL each. The 50 μL mixtures were subjected to amplification using an Eppendorf Thermocycler by 30 cycles, with 1 cycle at 94 °C for 1 min, at 34 °C for 2 min, and followed with a 7 min extension at 72 °C. Amplification of the 139-bp insert was confirmed by gel electrophoresis.

Construction of recombinant yCD variants

The DraIII and BglII sites in the vector backbone were removed by site-directed mutagenesis to construct the vector carrying the inactive or dummy gene,[47] using the oligonucleotide MB277 to remove the DraIII site and the oligonucleotide MB307 to remove the BglII site (Table 3). The yCD gene was inactivated by restriction with AccI followed by extension with the Klenow fragment and religation to reduce the presence of wild-type yCD in the selection. The resulting inactivated yCD was designated as 'pETHT:yCD-dummy.' Following digestion with BglII and DraIII, the gel-purified insert was cloned into the vector digested with the same restriction enzymes.

Transformation of E. coli GIA39(DE3) and positive selection

Approximately 3.5 μL of the ligated product was electroporated into 40 μL of electrocompetent *E. coli* GIA39(DE3) and then shaken at 37 °C for 1 h in 1 mL of SOC medium (3 g of bactopeptone, 2.5 g of yeast extract, 1 M NaCl, 1 M KCl, 5 mM $MgSO_4$, 5 mM $MgCl_2$, and 1.8% glucose per liter). The transformation mixture was concentrated by pelleting, resuspended in 100 μL of 0.9% NaCl, and plated at various volumes onto 2× YT rich medium and uracil and cytosine minimal media plates supplemented with 50 μg/mL of carbenicillin. Growth on cytosine minimal medium requires the presence of a functional yCD, while 2× YT and uracil minimal media were used as positive controls. Uracil minimal medium (500 mL) was prepared from 0.36 g of yeast synthetic dropout without leucine, 50 mL of 10× M9 salts (15 g of KH_2PO_4, 33.9 g of anhydrous $NaHPO_4$, 2.5 g of NaCl, and 5.0 g of NH_4Cl), 1 mM $MgSO_4$, 2.5 mL of 20% glucose, 0.1 mM $CaCl_2$, 1 mL of 2% leucine, and 7.5 g of bactoagar. Cytosine minimal medium (500 mL) was prepared from 1 mM cytosine, 0.96 g of yeast synthetic dropout without uracil, 8.5 g of bactoagar, 50 mL of 10× M9 salts, 1 mM $MgSO_4$, 2.5 mL of 20% glucose, and 0.1 mM $CaCl_2$. The 2× YT plates were incubated at 37 °C overnight, and the uracil and cytosine plates were incubated at 37 °C for approximately 36 h. The number of transformants on the 2× YT plate allows estimation of the library size. Transformants from the cytosine plates were picked and restreaked onto fresh cytosine plates to confirm the phenotype.

Selection of 5FC sensitive mutants

Genetic complementation of yCD was done as previously established for bCD.[48] The functional variants determined by the positive selection described above were streaked onto cytosine plates supplemented with 5FC at 10 μg/mL, a sublethal dose for wild-type yCD, and incubated for approximately 36 h at 37 °C to determine the

Table 3. List of oligonucleotides

Oligonucleotides used to generate the randomized DNA fragment[a]
MB223 (56mer), 5′ GTGAGATCTCCACTTTGGAAAACTGTGGGAGATTAGAGGGCAAA GTGTACAAAGAT 3′
MB224 (95mer), 5′ CCGACAA(CACAGCGTG)GAATACCATACATGAT**GATGGCACCTGT**ACA**CATGTC**GCATGG **AGACAG**CGT**CGTATACAAAGT**GGTATCTTTGTACAC 3′
MB225 (18mer), 5′ GTG(AGATCT)CCACTTTGG 3′
MB226 (17mer), 5′ CCGACAACACAGCGTGG 3′

Oligonucleotides used to introduce or eliminate restriction sites[b]
MB277 (21mer), 5′ CGATGGCCCAATACGTGAACC 3′
MB307 (22mer), 5′ CGGGATCGCGATCGCGGGCAGC 3′
MB374 (31mer), 5′ CGCTGTCTCCCATGCGA**A**ATGTGTACAGGTGC 3′
MB375 (31mer), 5′ CGACCTGTACACAT**T**TCGCATGGAGACAGCG 3′
MB376 (31mer), 5′ CGCTGTCTCCATGCGAC**C**TGTGTACAGGTGC 3′
MB377 (31mer), 5′ GCACCTGTACACA**G**GTCGCATGGAGACAGCG 3′
MB378 (34mer), 5′ GCGACATGTGTACAGGAGCC**C**TCATCATGTATGG 3′
MB379 (34mer), 5′ CCATACATGATGA**G**GGCTCCTGTACACATGTCGC 3′

[a] Nucleotides shown in bold are mixtures of wild-type nucleotides (79%) and the three non-wild-type nucleotides (21%). Parentheses denote the DraIII (MB224) and BglII (MB225) restriction sites used for cloning purposes.
[b] Nucleotides shown in bold were altered. Underlined nucleotides indicate change in restriction site.

ability of the mutants to confer 5FC sensitivity. Colonies unable to grow on the 5FC plates were selected from the control plates and subjected to additional rounds of negative selection at decreasing 5FC concentrations (5, 2, 1, and 0.5 μg/mL). Plasmid DNA of the yCD variants was isolated, and the randomized region was sequenced using the T7 terminator primer (5′ TATGCTAGTTATTGCTCAG 3′) at the core sequencing laboratory of Washington State University.

Construction of mammalian expression vectors

Computationally designed thermostabilized yCD genes described by Korkegian *et al.*[29] (pET15b:yCD-double and pET15b:yCD-triple) were subcloned into the mammalian expression vector pCDNA6/*myc*-His B (Invitrogen, Carlsbad, CA). The yCD-double and yCD-triple genes were subcloned into pCDNA6/*myc*-His B digested with EcoRV and XhoI as NcoI (blunt-ended)/XhoI fragments. After restriction enzyme verification, DNA sequencing analysis confirmed the presence of the yCD-double and yCD-triple genes.

Site-directed mutagenesis was performed to introduce the mutations derived from the regiospecific random mutagenesis to the yCD-triple mutant using a QuikChange site-directed mutagenesis kit from Stratagene according to the manufacturer's protocol. Three pairs of oligonucleotides containing the D92E (MB374/MB375-AflIII), M93L (MB376/MB377-AflIII), or I98L (MB378/MB379-BanI) substitution and a silent mutation to remove a restriction site for screening purposes were synthesized by Integrated DNA Technologies (Table 3). After restriction enzyme verification, DNA sequencing analysis was performed to confirm the presence of the correct mutation.

5FC sensitivity assays

One microgram of each DNA [pCDNA (vector alone), pCDNA:yCD, pCDNA:yCD-D92E, pCDNA:yCD-M93L, pCDNA:yCD-I98L, pCDNA:yCD-double, pCDNA:yCD-triple, pCDNA:yCD-triple/D92E, pCDNA:yCD-triple/M93L, and pCDNA:yCD-triple/I98L] was used to transfect 1×10^5 rat C6 glioma cells by lipofection using FuGENE 6 transfection reagent (Roche Diagnostics, Penzberg, Germany) at a 3:1 ratio according to the manufacturer's directions. Immunoblots were performed to assess protein expression. Briefly, pools of transfectants were harvested and resuspended at 100,000 cells/μL in lysis buffer [for 2 mL, 2 μL of 1 M DTT, 20 μL of 1 M Hepes, 40 μL of Nonidet P40 (Roche Diagnostics), 2 μL of $MgAc_2$, and H_2O to final volume). The resuspended pellets were incubated on ice for 20 min and subjected to centrifugation at 4 °C for 20 min to pellet debris. Heat-denatured samples (10 μL/well) were subjected to electrophoresis on 15% SDS-containing polyacrylamide gel, transferred to a nitrocellulose membrane, and blocked with 3% gelatin in Tris-buffered saline. The membrane was probed with rabbit polyclonal yCD antiserum (gift from Dr. Alnawaz Rehemtulla, University of Michigan, Ann Arbor, MI) followed by goat anti-rabbit alkaline phosphatase-conjugated antiserum. The blot was developed using the Alkaline Phosphatase Conjugate Substrate Kit (Bio-Rad, Hercules, CA). Pools of transfectants were transferred to 96-well microtiter plates at an initial density of 250 cells per well in Dulbecco's modified Eagle's medium plus supplements to determine the cytotoxicity of 5FC.[49] After cell adherence overnight, 5FC (0–10 mM) was added in sets of eight wells for each concentration tested. The plates were incubated for 6 days at 37 °C in 5% CO_2, at which time the redox-indicator dye Alamar Blue was added. Cell survival was determined several hours later according to the manufacturer's instructions, and the data were plotted with a standard error of the mean bar. At least three replicates were performed.

Xenograft tumor model

Pools of C6 glioma cells stably transfected with pCDNA, pCDNA:yCD, pCDNA:yCD-D92E, or pCDNA:yCD-triple (0.5×10^6 cells in 200 μL of PBS at pH 7.2) were injected subcutaneously into 5- to 6-week-old female nude mice ($n = 5$ for each group) (BALB/cAnNCr-*nu*/*nu*; National Cancer Institute, Frederick, MD). When the tumors reached 3–4 mm (day 0), PBS or 5FC (500 mg/kg) was administered by intraperitoneal injection once a day for 18 consecutive days. Starting on day 0, the tumor volume was monitored using caliper measurement (length, width, and height) every other day. Tumor volume was calculated using the following formula: $4/3\pi((\text{Width} \times \text{Length} \times \text{Height})/2)$. Tumor volume was plotted and analyzed for statistical significance using Student's *t* test.

Protein expression and purification

Protein expression and purification of yCD were carried out as previously described,[3] with the exception that buffer exchange was carried out with Bio-Rad prepacked Econo-Pac 10DG buffer exchange columns rather than overnight dialysis. Protein expression from pET15b:yCD (BL21-RIL) yields yCD with a thrombin-cleavable 6-His tag fused to the N-terminus. All kinetics and thermostability experiments were carried out with fresh, unfrozen protein stored at 4 °C for 2 weeks or less.

Activity assays

The conversion of cytosine to uracil by yCD was measured spectrophotometrically by monitoring change in absorbance at 286 nm, while the conversion of 5FC to 5FU was monitored at 238 nm.[29,48] The protein was diluted to 2 μM in 50 mM Tris–Cl, pH 7.5, and mixed 1:1 with a range of nine cytosine concentrations from 0.2–1 mM in the same buffer. Absorbance at 238 nm was measured every 5 s until baseline was reached, with the first reading taken 5 s after mixing. Measurements were taken in quadruplicate and averaged to reduce error. Initial velocity was calculated as a function of the initial slope by curve fitting the resulting plot, taking the derivative, and extrapolating back to time zero. K_m and k_{cat} values of wild-type yCD and mutant constructs were determined from a double-reciprocal (Lineweaver–Burk) plot of the resulting data, and the catalytic efficiency k_{cat}/K_m was calculated from these values.

Circular dichroism measurement and thermal denaturation experiments

Circular dichroism data were collected on an Aviv 62A DS spectrometer as described by Dantas *et al.*[50] Wavelength scans were run from 200 to 260 nm to determine the folded state of the protein, the ratio of concentration to signal strength, and the wavelength where signal strength

was at its highest. Temperature melts were run with 8–12 μM protein in a 2 mm path length cuvette from 10 to 98 °C in 2° increments, with temperature regulated by a Peltier device. Sample temperature was allowed to equilibrate for 30 s before measurement, and signal was collected and averaged over 30 s. Denaturation was recorded as a change in ellipticity over temperature. Apparent T_m values were determined by curve fitting.

Crystallization and structure determination

Crystals were grown using the methodology described by Ireton *et al.*[3] After 2 days, crystals appeared in the drops but were often twinned. These crystals were then used to streak seed into the clear lower-concentration drops where higher-quality crystals eventually grew. Crystals were looped out and soaked for 20 min in a mother liquor solution containing 2-hydroxypyrimidine concentrated 1.2:1 relative to protein. After soaking, the crystals were immediately transferred briefly to a cryo-buffer containing the 2-hydroxypyrimidine mother liquor plus 25% DMSO and then flash-frozen in liquid nitrogen. All data were collected from a single crystal on the 5.0.1 beamline at the Advanced Light Source synchrotron to 1.7 Å. Data were indexed and scaled using the DENZO/SCALEPACK program suite.[51] R_{merge} values for the higher-resolution scales were poor, and the data were thus re-indexed and scaled at 2.3 Å. The initial structures were generated by molecular replacement with the Evolutionary Programming for Molecular Replacement[52] using the wild-type yCD crystal structure with the mutated residues and any residues within a 4 Å shell of those residues truncated to alanine. Refinement was carried out in rounds using the program Crystallography & NMR System[53,54] with a random 10% of data withheld for cross-validation. The yCD-triple/D92E mutant crystal structure was refined at 2.3 Å to an R_{work}/R_{free} of 20.4/25.7. Electron density maps and models were visualized in XtalView,[55] while cartoon representations of the structure were generated using PyMOL [DeLano, W.L. (2002). The PyMOL Molecular Graphics System on the World Wide Web§].

PDB accession number

Coordinates and diffraction data for yCD-triple/D92E structure have been deposited in the PDB database with accession number 2o3k.

Acknowledgements

This work was supported by the National Institutes of Health through grants CA85939 (to M.E.B.), CA97328 (to B.L.S. and M.E.B.), and T32-GM08268 (to A.K.). We thank Dr. A. Rehemtulla for his gift of yCD antiserum.

References

1. Nishiyama, T., Kawamura, Y., Kawamoto, K., Matsumura, H., Yamamoto, N., Ito, T. *et al.* (1985). Antineoplastic effects in rats of 5-fluorocytosine in combination with cytosine deaminase capsules. *Cancer Res.* **45**, 1753–1761.
2. Ireton, G., McDermitt, G., Black, M. E. & Stoddard, B. L. (2002). The structure of *Escherichia coli* cytosine deaminase. *J. Mol. Biol.* **315**, 687–697.
3. Ireton, G. C., Black, M. E. & Stoddard, B. L. (2003). The 1.14 Å crystal structure of yeast cytosine deaminase: evolution of nucleotide salvage enzymes and implications for genetic chemotherapy. *Structure (Camb.)*, **11**, 961–972.
4. Huber, B. E., Richards, C. A. & Krenitsky, T. A. (1991). Retroviral-mediated gene therapy for the treatment of hepatocellular carcinoma: an innovative approach for cancer therapy. *Proc. Natl Acad. Sci. USA*, **88**, 8039–8043.
5. Kanamaru, R., Kakuta, H., Sato, T., Ishioka, C. & Wakui, A. (1986). The inhibitory effects of 5-fluorouracil on the metabolism of preribosomal and ribosomal RNA in L-1210 cells *in vitro*. *Cancer Chemother. Pharmacol.* **17**, 43–46.
6. Pinedo, H. M. & Peters, G. F. (1988). Fluorouracil: biochemistry and pharmacology. *J. Clin. Oncol.* **6**, 1653–1664.
7. Thomas, D. M. & Zalcberg, J. R. (1998). 5-fluorouracil: a pharmacological paradigm in the use of cytotoxics. *Clin. Exp. Pharmacol. Physiol.* **25**, 887–895.
8. Kaliberov, S. A., Market, J. M., Gillespie, G. Y., Krendelchtchikova, V., Della Manna, D., Sellers, J. C. *et al.* (2007). Mutation of *Escherichia coli* cytosine deaminase significantly enhances molecular chemotherapy of human glioma. *Gene Ther.* **14**, 1111–1119.
9. Hiraoka, K., Kimura, T., Logg, C. R., Tai, C. K., Haga, K., Lawson, G. W. & Kasahara, N. (2007). Therapeutic efficacy of replication-competent retrovirus vector-mediated suicide gene therapy in a multifocal colorectal cancer metastasis model. *Cancer Res.* **67**, 5345–5353.
10. Liu, Y., Ye, T., Maynard, J., Akbulut, H. & Deisseroth, A. (2006). Engineering conditionally replication-competent adenoviral vectors carrying the cytosine deaminase gene increases the infectivity and therapeutic effect for breast cancer gene therapy. *Cancer Gene Ther.* **13**, 346–356.
11. Freytag, S. O., Movsas, B., Aref, I., Stricker, H., Peabody, J., Pegg, J. *et al.* (2007). Phase I trial of replication-competent adenovirus-mediated suicide gene therapy combined with IMRT for prostate cancer. *Mol. Ther.* **15**, 1016–1023.
12. Post, D. E., Shim, H., Toussaint-Smith, E. & Van Meir, E. G. (2005). Cancer Scene Investigation: how a cold virus became a tumor killer. *Future Oncol.* **1**, 247–258.
13. Barton, K. N., Paielli, D., Zhang, Y., Koul, S., Brown, S. L., Lu, M. *et al.* (2006). Second-generation replication-competent oncolytic adenovirus armed with improved suicide genes and ADP gene demonstrates greater efficacy without increased toxicity. *Mol. Ther.* **13**, 347–356.
14. Freytag, S. O., Stricker, H., Pegg, J., Paielli, D., Pradhan, D. G., Peabody, J. *et al.* (2003). Phase I study of replication-competent adenovirus-mediated double-suicide gene therapy in combination with conventional-dose three-dimensional conformal radiation therapy for the treatment of newly diagnosed, intermediate- to high-risk prostate cancer. *Cancer Res.* **63**, 7497–7506.
15. Freytag, S. O., Khil, M., Stricker, H., Peabody, J., Menon, M., DePeralta-Venturina, M. *et al.* (2002). Phase I study of replication-competent adenovirus-

§ http://www.pymol.org

mediated double suicide gene therapy for the treatment of locally recurrent prostate cancer. *Cancer Res.* **62**, 4968–4976.
16. Diasio, R. B., Laking, D. E. & Bennett, J. E. (1978). Evidence for conversion of 5-fluorocytosine to 5-fluorouracil in humans: possible factor in 5-fluorocytosine clinical toxicity. *Antimicrob. Agents Chemother.* **14**, 903–908.
17. Lawrence, T. S., Rehemtulla, A., Ng, E. Y., Wilson, M., Trosko, J. E. & Stetson, P. L. (1998). Preferential cytotoxicity of cells transduced with cytosine deaminase compared to bystander cells after treatment with 5-flucytosine. *Cancer Res.* **58**, 2588–2593.
18. Hoganson, D. K., Batra, R. K., Olsen, J. C. & Boucher, R. C. (1996). Comparison of the effects of three different toxin genes and their levels of expression on cell growth and bystander effect in lung adenocarcinoma. *Cancer Res.* **56**, 1315–1323.
19. Kuriyama, S., Masui, K., Sakamoto, T., Nakatani, T., Kikukawa, M., Tsujinoue, H. *et al.* (1998). Bystander effect caused by cytosine deaminase gene and 5-fluorocytosine *in vitro* is substantially mediated by generated 5-fluorouracil. *Anticancer Res.* **18**, 3399–3406.
20. Nishihara, E., Nagayama, Y., Narimatsu, M., Namba, H., Watanabe, M., Niwa, M. & Yamashita, S. (1998). Treatment of thyroid carcinoma cells with four different suicide gene/prodrug combinations *in vitro*. *Anticancer Res.* **18**, 1521–1525.
21. Trinh, Q. T., Austin, E. A., Murray, D. M., Knick, V. C. & Huber, B. E. (1995). Enzyme/prodrug gene therapy: comparison of cytosine deaminase/5-fluorocytosine *versus* thymidine kinase/ganciclovir enzyme/prodrug systems in a human colorectal carcinoma cell line. *Cancer Res.* **55**, 4808–4812.
22. Kievit, E., Nyati, M. K., Ng, E., Stegman, L. D., Parsels, J., Ross, B. D. *et al.* (2000). Yeast cytosine deaminase improves radiosensitization and bystander effect by 5-fluorocytosine of human colorectal cancer xenografts. *Cancer Res.* **60**, 6649–6655.
23. Lawrence, T. S., Davis, M. A. & Maybaum, J. (1994). Dependence of 5-fluorouracil-mediated radiosensitization on DNA-directed effects. *Int. J. Radiat. Oncol., Biol., Phys.* **29**, 519–523.
24. Hamstra, D. A., Rice, D. J., Pu, A., Oyedijo, D., Ross, B. D. & Rehemtulla, A. (1999). Combined radiation and enzyme/prodrug treatment for head and neck cancer in an orthotopic animal model. *Radiat. Res.* **152**, 499–507.
25. Stackhouse, M. A., Pederson, L. C., Grizzle, W. E., Curiel, D. T., Gebert, J., Haack, K. *et al.* (2000). Fractionated radiation therapy in combination with adenoviral delivery of the cytosine deaminase gene and 5-fluorocytosine enhances cytotoxic and antitumor effects in human colorectal and cholangiocarcinoma models. *Gene Ther.* **7**, 1019–1026.
26. Yao, L., Li, Y., Wu, Y., Liu, A. & Yan, H. (2005). Product release is rate-limiting in the activation of the prodrug 5-fluorocytosine by yeast cytosine deaminase. *Biochemistry*, **44**, 5940–5947.
27. Kievit, E., Bershad, E., Ng, E., Sethna, P., Dev, I., Lawrence, T. S. & Rehemtulla, A. (1999). Superiority of yeast over bacterial cytosine deaminase for enzyme/prodrug gene therapy in colon cancer xenografts. *Cancer Res.* **59**, 1417–1421.
28. Katsuragi, T., Sakai, T. & Tonomura, K. (1987). Implantable enzyme capsules for cancer chemotherapy from bakers' yeast cytosine deaminase immobilized on epoxy–acrylic resin and urethane prepolymer. *Appl. Biochem. Biotechnol.* **16**, 61–69.
29. Korkegian, A., Black, M. E., Baker, D. & Stoddard, B. L. (2005). Computational thermostabilization of an enzyme. *Science*, **308**, 857–860.
30. Davies, G. J., Gamblin, S. J., Littlechild, J. A. & Watson, H. C. (1993). The structure of a thermally stable 3-phosphoglycerate kinase and a comparison with its mesophilic equivalent. *Proteins: Struct. Funct. Genet.* **15**, 283–289.
31. Yip, K. S., Stillman, T. J., Britton, K. L., Artymiuk, P. J., Baker, P. J., Sedelnikova, S. E. *et al.* (1995). The structure of *Pyrococcus furiosus* glutamate dehydrogenase reveals a key role for ion-pair networks in maintaining enzyme stability at extreme temperatures. *Structure*, **3**, 1147–1158.
32. Rice, D. W., Yip, K. S., Stillman, T. J., Britton, K. L., Fuentes, A., Connerton, I. *et al.* (1996). Insights into the molecular basis of thermal stability from the structure determination of *Pyrococcus furiosus* glutamate dehydrogenase. *FEMS Microbiol. Rev.* **18**, 105–117.
33. Harris, G. W., Pickersgill, R. W., Connerton, I., Debeire, P., Touzel, J. P., Breton, C. & Perez, S. (1997). Structural basis of the properties of an industrially relevant thermophilic xylanase. *Proteins: Struct. Funct. Genet.* **29**, 77–86.
34. Wallon, G., Kryger, G., Lovett, S. T., Oshima, T., Ringe, D. & Petsko, G. A. (1997). Crystal structures of *Escherichia coli* and *Salmonella typhimurium* 3-isopropylmalate dehydrogenase and comparison with their thermophilic counterpart from *Thermus thermophilus*. *J. Mol. Biol.* **266**, 1016–1031.
35. Russell, R. J., Ferguson, J. M., Hough, D. W., Danson, M. J. & Taylor, G. L. (1997). The crystal structure of citrate synthase from the hyperthermophilic archaeon *Pyrococcus furiosus* at 1.9 Å resolution. *Biochemistry*, **36**, 9983–9994.
36. Baker, D., Sohl, J. L. & Agard, D. A. (1992). A protein folding reaction under kinetic control. *Nature*, **356**, 263–265.
37. Kelch, B. A. & Agard, D. A. (2007). Mesophile *versus* thermophile: insights into the structural mechanisms of kinetic stability. *J. Mol. Biol.* **370**, 784–795.
38. Dachs, G. U., Tupper, J. & Tozer, G. M. (2005). From bench to bedside for gene-directed enzyme prodrug therapy of cancer. *Anticancer Drugs*, **16**, 349–359.
39. Norris, J. S., Norris, K. L., Holman, D. H., El-Zawahry, A., Keane, T. E., Dong, J. Y. & Tavassoli, M. (2005). The present and future for gene and viral therapy of directly accessible prostate and squamous cell cancers of the head and neck. *Future Oncol.* **1**, 115–123.
40. Black, M. E., Kokoris, M. S. & Sabo, P. (2001). Herpes simplex virus-1 thymidine kinase mutants created by semi-random sequence mutagenesis improve prodrug-mediated tumor cell killing. *Cancer Res.* **61**, 3022–3026.
41. Wiedrodt, R., Amin, K., Kiefer, M., Jovanovic, V. P., Kapoor, V., Force, S. *et al.* (2003). Adenovirus-mediated gene transfer of enhanced herpes simplex virus thymidine kinase mutants improves prodrug-mediated tumor cell killing. *Cancer Gene Ther.* **10**, 353–364.
42. Rogulski, K. R., Kim, J. H., Kim, S. H. & Freytag, S. O. (1997). Glioma cells transduced with an *Escherichia coli* CD/HSV-1 TK fusion gene exhibit enhanced metabolic suicide and radiosensitivity. *Hum. Gene Ther.* **8**, 73–85.
43. Erbs, P., Regulier, E., Kintz, J., Leroy, P., Poitevin, Y., Exinger, F. *et al.* (2000). *In vivo* cancer gene therapy by adenovirus-mediated transfer of a bifunctional yeast cytosine deaminase/uracil phosphoribosyltransferase fusion gene. *Cancer Res.* **60**, 3813–3822.

44. Adachi, Y., Tamiya, T., Ichikawa, T., Terada, K., Ono, Y., Matsumoto, K. *et al.* (2000). Experimental gene therapy for brain tumors using adenovirus-mediated transfer of cytosine deaminase gene and uracil phosphoribosyltransferase gene with 5-fluorocytosine. *Hum. Gene Ther.* **11**, 77–89.
45. Willmon, C. L., Krabbenhoft, E. & Black, M. E. (2006). A guanylate kinase/HSV-1 thymidine kinase fusion protein enhances prodrug-mediated cell killing. *Gene Ther.* **13**, 1309–1312.
46. Kurtz, J. E. & Black, M. E. (2004). Enhancement of suicide gene prodrug activation by random mutagenesis. *Methods Mol. Med.* **90**, 331–344.
47. Kunkel, T. A., Roberts, J. D. & Zakour, R. A. (1987). Rapid and efficient site-specific mutagenesis without phenotypic selection. *Methods Enzymol.* **154**, 367–382.
48. Mahan, S. D., Ireton, G. C., Stoddard, B. L. & Black, M. E. (2004). Alanine-scanning mutagenesis reveals a cytosine deaminase mutant with altered substrate preference. *Biochemistry*, **43**, 8957–8964.
49. Kokoris, M. S., Sabo, P., Adman, E. T. & Black, M. E. (1999). Enhancement of tumor ablation by a selected HSV-1 thymidine kinase mutant. *Gene Ther.* **6**, 1415–1426.
50. Dantas, G., Kuhlman, B., Callender, D., Wong, M. & Baker, D. (2003). A large scale test of computational protein design: folding and stability of nine completely redesigned globular proteins. *J. Mol. Biol.* **332**, 449–460.
51. Otwinowski, Z. & Minor, W. (1997). Processing of x-ray diffraction data collected in oscillation mode. *Methods Enzymol.* **276**, 307–326.
52. Kissinger, C. R., Gehlhaar, D. K. & Fogel, D. B. (1999). Rapid automated molecular replacement by evolutionary search. *Acta Crystallogr., Sect. D: Biol. Crystallogr.* **55**, 484–491.
53. Brunger, A. T. (1993). Assessment of phase accuracy by cross validation: the free *R* value. Methods and applications. *Acta Crystallogr., Sect. D: Biol. Crystallogr.* **49**, 24–36.
54. Brunger, A. T., Adams, P. D., Clore, G. M., DeLano, W. L., Gros, P., Grosse-Kunstleve, R. W. *et al.* (1998). Crystallography & NMR System: a new software suite for macromolecular structure determination. *Acta Crystallogr., Sect. D: Biol. Crystallogr.* **54**, 905–921.
55. McRee, D. E. (1992). A visual protein crystallographic software system for X11/XView. *J. Mol. Graphics*, **10**, 44–46.